Carbohydrate Polymers 81 (2010) 284–290

Contents lists available at ScienceDirect

Carbohydrate Polymers

journal homepage: www.elsevier.com/locate/carbpol

Effect of solvent on the adsorption behavior and on the surface properties of *Sterculia striata* polysaccharide

Aline F. Dario[a], Regina C.M. de Paula[b], Haroldo C.B. Paula[c], Judith P.A. Feitosa[b], Denise F.S. Petri[a,*]

[a] *Instituto de Química, Universidade de São Paulo, Av. Prof. Lineu Prestes 748, 05508-000 São Paulo, SP, Brazil*
[b] *Departamento de Química Inorgânica e Orgânica, Universidade Federal do Ceará, Fortaleza – CE, Brazil*
[c] *Departamento de Química Analítica e Fisico-Química, Universidade Federal do Ceará, Fortaleza – CE, Brazil*

ARTICLE INFO

Article history:
Received 16 November 2009
Received in revised form 10 February 2010
Accepted 11 February 2010
Available online 4 March 2010

Keywords:
Sterculia striata polysaccharide
Surface energy
Ionic liquid
Lysozyme

ABSTRACT

Characterization of *Sterculia striata* polysaccharide (SSP) films adsorbed onto Si wafers from solutions prepared in ethyl methyl imidazolium acetate (EmimAc), water or NaOH 0.01 mol/L was systematically studied by means of ellipsometry, atomic force microscopy and contact angle measurements. SSP adsorbed from EmimAc onto Si wafer as homogeneous monolayers (~0.5 nm thick), while from water or NaOH 0.01 mol/L SSP formed layers of ~4.0 nm and ~1.5 nm thick, respectively. Surface energy values found for SSP adsorbed from EmimAc or water were 68 ± 2 mJ/m^2 and 65 ± 2 mJ/m^2, respectively, whereas from NaOH it amounted to 57 ± 3 mJ/m^2. The immobilization of lysozyme (LYS) onto SSP films was also investigated. The mean thickness of LYS (d_{LYS}) immobilized onto SSP films adsorbed from each solvent tended to increase with the decrease of γ_S^p and γ_S^{total}. However, the enzymatic activity of LYS molecules was higher when they were immobilized onto SSP films with higher γ_S^p and γ_S^{total} values.

© 2010 Elsevier Ltd. All rights reserved.

1. Introduction

Polysaccharides are interesting materials for the fabrication of thin films because they can be obtained from renewable sources, they are biocompatible materials and recognized by many biomolecules. Such characteristics make polysaccharides potential materials for the development of biotechnological devices. On the other hand, the strong intermolecular interactions among polysaccharide chains reduce their solubility, making their processing a big challenge. During the last decade ionic liquids (ILs) have been used as solvents for polysaccharides (Swatloski, Spear, Holbrey, & Rogers, 2002). Often solubilization and derivatization of polysaccharides occur at high temperatures, turning the use of a lot of common solvents forbidden because of their boiling points. Thus, the use of ILs, which have high thermal stability, low melting point and low vapor pressure, represents a large advantage in relation to other solvents (El Seoud, Koschella, Fidale, Dorn, & Heinze, 2007).

The characteristics (thickness, morphology) and properties (surface energy) of thin polymer films deposited from solutions onto a given substrate depend on the interactions between substrate and polymer, substrate and solvent, and polymer and solvent. For instance, the effect of the substrate and solvent on the thickness, surface energy and morphology of cellulose (Kontturi et al., 2007) or cellulose ester (Amim Júnior, Petri, Maia, & Miranda, 2009; Amim Júnior, Kosaka, Petri, Maia, & Miranda, 2009) thin films has been recently reported.

Polysaccharide from *Sterculia striata* (SSP), which belongs to the same family of karaya polysaccharide, contains (mol%) rhamnose (23.8–28.8), galactose (19.3–23.4), xylose (5.6–7.7), uronic acid (42.2–49.2), and acetyl groups (9.6–10.7) (Brito, Sierakowski, Reicher, Paula, & Feitosa, 2005; Brito, Silva, Paula, & Feitosa, 2004). This polysaccharide forms thermoreversible gels with gelation conditions depending on the purification method, acetyl group's content and presence of salt (Silva, Brito, Paula, Feitosa, & Paula, 2003). The high content of uronic acid groups in the SSP chains allowed their application in the build-up of electroactive nanocomposites (Zampa et al., 2007). In the present study, the effect of the solvent used for SSP adsorption onto Si wafers on the resulting films surface properties and characteristics was investigated. Ethyl methyl imidazolium acetate (EmimAc), an ionic liquid, water, mixtures of EmimAc with different contents of water and NaOH 0.01 mol/L were used as solvents for SSP. Surface properties were determined by means of contact angle measurements and films thickness and morphology were determined by means of ellipsometry and atomic force microscopy (AFM). The dependence of enzyme adsorption on the SSP surface properties was also investigated. Lysozyme was chosen for these experiments due to its antimicrobial functions (McKenzie & White, 1991).

* Corresponding author. Tel.: +55 11 30913831; fax: +55 11 38155579.
E-mail addresses: dfsp@iq.usp.br, dfsp@usp.br (D.F.S. Petri).

0144-8617/$ – see front matter © 2010 Elsevier Ltd. All rights reserved.
doi:10.1016/j.carbpol.2010.02.015

Table 1
Advancing contact angle measurements for SSP films adsorbed from pure EmimAc, pure water, and NaH 0.01 mol/L onto Si wafers with drops of diiodomethane (θ_D) and water (θ_W) as test liquids. Films mean roughness (rms) and mean thickness (d) values are also indicated. Dispersive (γ_S^d) and polar (γ_S^p) components of the surface energy were determined for SSP using the geometric* and harmonic-mean** equations.

Solvent	d (nm)	rms (nm)	θ_D (°)	θ_W (°)	$^*\gamma_S^d$ (mJ/m^2)	$^*\gamma_S^p$ (mJ/m^2)	$^*\gamma_S^{total}$ (mJ/m^2)	$^{**}\gamma_S^d$ (mJ/m^2)	$^{**}\gamma_S^p$ (mJ/m^2)	$^{**}\gamma_S^{total}$ (mJ/m^2)
EmimAc	0.5 ± 0.1	0.18 ± 0.03	41 ± 1	31 ± 2	39 ± 2	29 ± 1	68 ± 2	40 ± 2	32 ± 2	72 ± 2
Water	3.8 ± 0.9	0.24 ± 0.04	40 ± 1	39 ± 1	40 ± 2	25 ± 2	65 ± 2	40 ± 2	28 ± 2	68 ± 2
NaOH 0.01 mol/L	1.4 ± 0.2	1.20 ± 0.1	34 ± 1	55 ± 1	43 ± 3	14 ± 2	57 ± 3	43 ± 4	20 ± 2	63 ± 6

2. Experimental

S. striata polysaccharide (SSP) was purified and characterized as described elsewhere (Brito et al., 2004, 2005). Pure ionic liquid 1-etyl-3-metyl-imidazolium acetate (EmimAc, Sigma, 51053, BasionicTM BC01), mixtures of EmimAc and water (20/80, 30/70, 50/50, 70/30, 80/20, 90/10 in volume) and NaOH 0.01 mol/L solution were used as solvents. The concentration of SSP in solution was kept constant at 1.0 g/L. Solubility of SSP in these solvents was evaluated by means of turbidity determined from transmittance at 650 nm using a Beckmann Coulter DU-600 spectrophotometer at 25 °C. For each measurement the corresponding solvent was used as blank.

Si wafers (University Wafer, MA, USA) with native top SiO_2 layer and 1.0 cm^2 area were rinsed in an oxidative solution (NH_4OH, H_2O_2 and water) at 75 °C, as described elsewhere (Petri, Wenz, Schunk, & Schimmel, 1999), and characterized by means of ellipsometry. Lysozyme from chicken egg white (LYS, E.C. 3.2.1.17, Sigma L7651, Lot 096K1237) was dissolved in NaCl 0.01 mol/L (pH 6.5) at 1.0 g/L.

Adsorption studies of SSP onto Si wafers were carried out by dipping clean Si wafers in the polymer solution for a period of 30 min at 70 ± 1 °C. Such conditions were optimized in order to obtain thin adsorbed layers. After that the samples were exhaustively rinsed with distilled water in order to remove physically adsorbed molecules (solvent or SSP chains) from the surface. The adsorption of LYS was studied by immersing SSP-covered Si wafers in the enzyme solution during 3 h at 24 ± 1 °C. After each adsorption experiment, samples were exhaustively rinsed with distilled water and dried under a stream of N_2.

Ellipsometric measurements were performed in air using a vertical computer-controlled DRE-EL02 ellipsometer (Ratzeburg, Germany). The angle of incidence was set at 70.0° and the wavelength, λ, of the He–Ne laser was 632.8 nm. For data interpretation, a multilayer model composed of the substrate, the unknown layer, and the surrounding medium were used. The thickness, d_x, and refractive index, n_x, of the unknown layer were calculated from the ellipsometric angles, Δ and Ψ, using the fundamental ellipsometric equation and iterative calculations with Jones matrices (Azzam & Bashara, 1987):

$$e^{i\Delta} \cdot \tan\Psi = \frac{R_p}{R_s} = f(n_x, d_x, \lambda, \phi) \quad (1)$$

where R_p and R_s are the overall reflection coefficients for the parallel and perpendicular waves. They are functions of the angle of incidence, ϕ, the wavelength, λ, of the radiation, and of the refractive index and thickness of each layer of the model, n_x and d_x, respectively.

From the ellipsometric angles, Δ and Ψ, and a multilayer model composed of silicon, silicon dioxide, polysaccharide layer, and air, it is possible to determine only the thickness of the polysaccharide layer, d_{poly}. The thickness of the silicon dioxide layers was determined in air, assuming a refractive index of 3.88–0.018i and infinite thickness for silicon (Palik, 1985). The refractive index for the surrounding medium (air) was taken as 1.00. Because the native silicon dioxide layer is very thin, its refractive index was taken as 1.462 (Palik, 1985) and only the thickness was calculated. The mean thickness of the native silicon dioxide layer was 2.0 ± 0.2 nm. After determining the thickness of the silicon dioxide layer, the mean thickness of adsorbed SSP layers was determined in air by means of ellipsometry, considering the refractive index of 1.50. The mean thickness of adsorbed LYS onto SSP films was determined, considering the refractive index of 1.52 (Ortega-Vinuesa, Tengvall, & Lundstrom, 1998).

2.1. Contact angle measurements

Contact angle θ measurements were performed at 24 ± 1 °C in a home-built apparatus (Adamson, 1990) using sessile drops of 8 μL. In order to determine the surface energy of the polymers (γ_S), contact angle θ measurements were performed with diiodomethane (>99.5%, purely dispersive nature) and distilled water (polar liquid). In order to use Young's equation without correction for roughness and chemical heterogeneity (Marmur, 2006), only very smooth and homogeneous films were used. At least three films of the same sample were analyzed. The polar (γ_S^p) and dispersive (γ_S^d) components of the surface energy of PSS were determined by Owens–Wendt's (Owens & Wendt, 1969) equation, also known as geometric mean equation, and by harmonic-mean equation.

Atomic force microscopy (*AFM*) analyses were performed with a PICO SPM-LE (Molecular Imaging) microscope in intermittent contact mode in air at room temperature, using silicon cantilevers with a resonance frequency close to 300 kHz. Areas ranging from 2 μm × 2 μm to 1 μm × 1 μm were scanned with a resolution of 512 × 512 pixels. Image processing and the determination of the root mean square (rms) roughness were performed using the Pico Scan software. At least two films of the same composition were analyzed in different areas of the surface.

Evaluation of antimicrobial effect of immobilized LYS onto SSP films was performed at 25 °C, using aqueous dispersions of *micrococcus luteus* (ATCC 4698) at 1.33 g/L as substrate (Bergmeyer, 1984). The activity was assessed by the relative turbidity decrease ($\Delta\tau$) determined from transmittance at 650 nm using a Beckmann Coulter DU-600 spectrophotometer at 25 °C just after the dispersion preparation (τ_0). Then three samples containing immobilized LYS onto SSP (total area of 3.0 cm^2) were put in contact with 5 mL of microorganism dispersion during 1 h. After that period of time, turbidity of supernant dispersions was measured again (τ). Bacteria disruption indicated antimicrobial activity (Bergmeyer, 1984) and was correlated with the relative decrease of turbidity ($\Delta\tau$):

$$\Delta\tau = \frac{\tau_0 - \tau}{\tau_0} \times 100\% \quad (2)$$

The larger is $\Delta\tau$, the more efficient is the antimicrobial agent. In order to check the possibility of re-use of immobilized LYS onto SSP films, after turbidimetric measurements samples were rinsed with distilled water, dried under a stream of N_2 and stored in the laboratory environment for 24 h. In the next day the antimicrobial tests were repeated with the same samples under the same conditions. All samples were characterized by means of ellipsometry and AFM prior to biocidal tests.

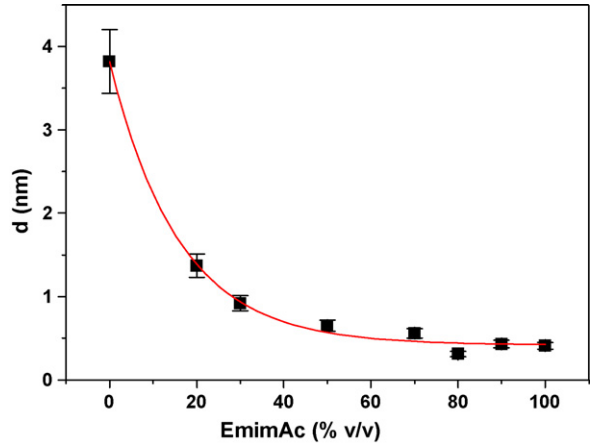

Fig. 1. Dependence of mean thickness values (d) of adsorbed SSP from solution (1.0 g/L) onto Si/SiO_2 wafers as a function of EmimAc content in the solution. The adsorption time and temperature were 30 min and 70 ± 1 °C, respectively. The solid line represents an exponential fit.

3. Results and discussion

Fig. 1 shows the ellipsometric mean thickness (d) of SSP adsorbed onto Si/SiO_2 as a function of EmimAc content in the solution. The thickest layer (3.8 ± 0.9) nm was obtained in pure water. For comparison, the thickness of a cellulose monolayer amounts to 0.7 nm (Wiegand, Jaworek, Wegner, & Sackmann, 1997). Therefore, the thick SSP layer probably corresponds to multilayers. However, the mean thickness values (d) decreased exponentially with the increase of EmimAc content in the solution, reaching a plateau value of 0.45 ± 0.05 nm for EmimAc contents higher than 70% in volume. This plateau value might be attributed to the adsorption of a polysaccharide monolayer. The solubility of SSP in EmimAc is favored by ionic and ion-dipole interaction, leading to the complete dissolution of the polysaccharide. The interactions between SSP and water are ion–dipole and dipole–dipole type, which are weaker than those between SSP and EmimAc (electrostatic and ion–dipole). Fig. 2 shows that turbidity decreased exponentially with the increase of EmimAc content in the solution, indicating that pure EmimAc is a better solvent than pure water and corroborating with adsorption behavior.

AFM topographic images showed that SSP adsorbed from pure EmimAc (Fig. 3a) or pure water (Fig. 3b) formed layers with rms = 0.18 ± 0.03 nm and rms = 0.24 ± 0.04 nm, respectively. The surface in Fig. 3a is very smooth with very few spherical particles distributed on the surface. Tiny globules well packed were observed for SSP adsorbed layers from pure water (Fig. 3b) or from EmimAc/water mixtures (Fig. 3c). Such morphology might be due to drying process and to the polymer concentration. When SSP adsorbed onto Si wafers from a more diluted solution (0.05 g/L) prepared either in pure EmimAc or in pure water, the mean thickness decreased to 0.20 ± 0.04 nm. AFM images evidenced that this low mean thickness value corresponds to isolated SSP molecules (Fig. 4) when the polymer solution was prepared in EmimAc or to small aggregates sparsely distributed on the surface when water was used as solvent (images not shown). The isolated SSP chains are between 0.4 nm and 0.7 nm high (cross-section in Fig. 4), such dimension could be correlated with polysaccharides backbone (Dumitriu, 2005). These findings indicated that EmimAc dissolves SSP at the molecular level and that polymer concentration at 1.0 g/L is enough to cover homogeneously the Si wafers.

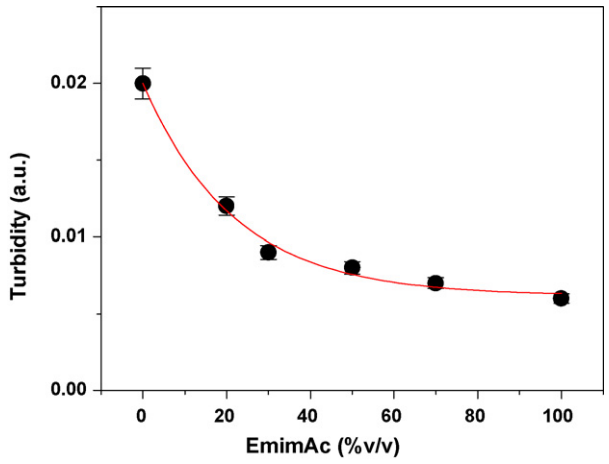

Fig. 2. Turbidity measured at 25 ± 1 °C for SSP solutions (1.0 g/L) as a function of EmimAc content in the solution. The solid line represents an exponential fit.

The adsorption of SSP onto Si wafers from NaOH 0.01 mol/L (pH 12) at 1.0 g/L was also investigated because alkaline conditions often favor polysaccharide dissolution. The mean thickness of adsorbed SSP layer amounted to 1.4 ± 0.2 nm. AFM image in Fig. 3d shows SSP chains arranged into spherical entities on the surface, yielding rms value of 1.2 ± 0.1 nm. Solutions of SSP were also prepared in NaOH 0.1 mol/L (pH 13) and 1.0 mol/L (pH 14) in order to verify if dissolution of SSP into individual chains could be achieved and if isolated chains could adsorb onto Si wafers. At pH 13 and pH 14 the mean d values of SSP adsorbed onto Si wafers amounted to 6 ± 1 nm and 21 ± 3 nm, respectively, indicating aggregation. The corresponding AFM images confirmed the presence of large aggregates (Supplementary Material). The good solubility of SSP solutions prepared at pH 12, 13 and 14 was attested by the very low turbidity values 0.007, 0004 and 0.002, respectively. Therefore, aggregation observed in the AFM images was probably induced by the SSP chains already adsorbed onto Si wafers.

In order to determine the surface energy of SSP films adsorbed from different solvents only flat and homogeneous films were chosen. Films mean roughness and mean thickness values are given in Table 1. Advancing contact angles, θ, determined for drops of water and diiodomethane on SSP films, the dispersive (γ_S^d) and polar (γ_S^p) components of the surface energy were calculated for SSP adsorbed from each solvent, as shown in Table 1. The sum of γ^d and γ^p gives the total surface energy (γ^{total}), as proposed by Fowkes (Chaudhury, 1996).

The surface energy γ_S^{total} values calculated for SSP films by means of harmonic-mean equation was (5–10%) higher than those determined with geometric model, as shown in Table 1. Similar tendency was also observed for low surface energy polymers, as polypropylene and polystyrene (Shimizu & Demarquette, 2000). SSP films adsorbed from EmimAc presented the highest surface energy value 68 ± 2 mJ/m^2 and 72 ± 2 mJ/m^2. The latter was as high as the surface tension of distilled water! Although polysaccharides are hydroxyl rich polymers, it is difficult to consider the same magnitude of intermolecular H bonding as in liquid water. A possible reason for this high surface energy value might be residual EmimAc molecules, which remained attached to the SSP films even after exhaustively rinsing with distilled water. Moreover, the surface energy values determined with harmonic model might be overestimated and from this point on the discussion will be focused only on the surface energy values determined with geometric model. Surface energy values calculated for SSP films adsorbed onto Si wafers from EmimAc, water and NaOH 0.01 mol/L amounted to 68 ± 2 mJ/m^2, 65 ± 2 mJ/m^2 and 57 ± 2 mJ/m^2, respectively. The dispersive component γ_S^d dominated the γ_S^{total} values. Similar values were found for cellulose nanocrystals spin coated from acidic solution onto Si wafers ~65 mJ/m^2, 31 mJ/m^2, and 34 mJ/m^2, for γ_S^{total}, γ_S^p and γ_S^d, respectively (Kontturi et al., 2007). In the case of SSP

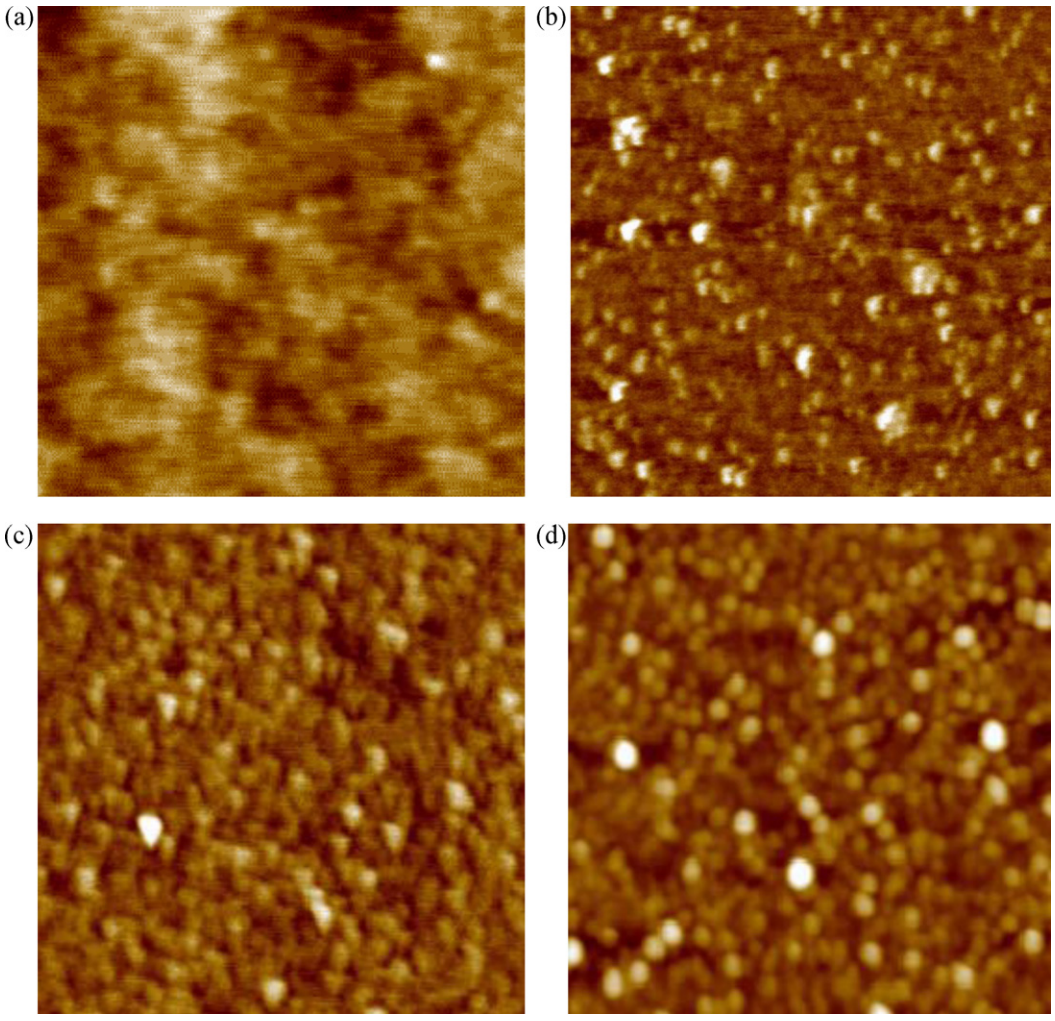

Fig. 3. AFM topographic images (1 μm × 1 μm) of SSP adsorbed onto Si wafers from solution (1.0 g/L) prepared in (a) pure EmimAc, Z = 2.0 nm; (b) pure water, Z = 3.0 nm; (c) mixture of EmimAc/water (10/90), Z = 3.0 nm and (d) NaOH 0.01 mol/L, Z = 15.0 nm.

adsorbed from EmimAc and water the γ_S^{total} and the components γ_S^p and γ_S^d were similar, although EmimAc seems to be a better solvent for SSP than water (Fig. 1). However, SSP films adsorbed from NaOH 0.01 mol/L presented low γ_S^p value, which decreased the γ_S^{total} value.

Biocompatibility of polysaccharides surfaces makes them interesting materials for biotechnological devices. However, surface energy parameters seem to control the adhesion and growth of cells (Gomes et al., 2007; Harnett, Alderman, & Wood, 2007) or the adsorption of proteins (Kosaka, Kawano, El Seoud, & Petri,

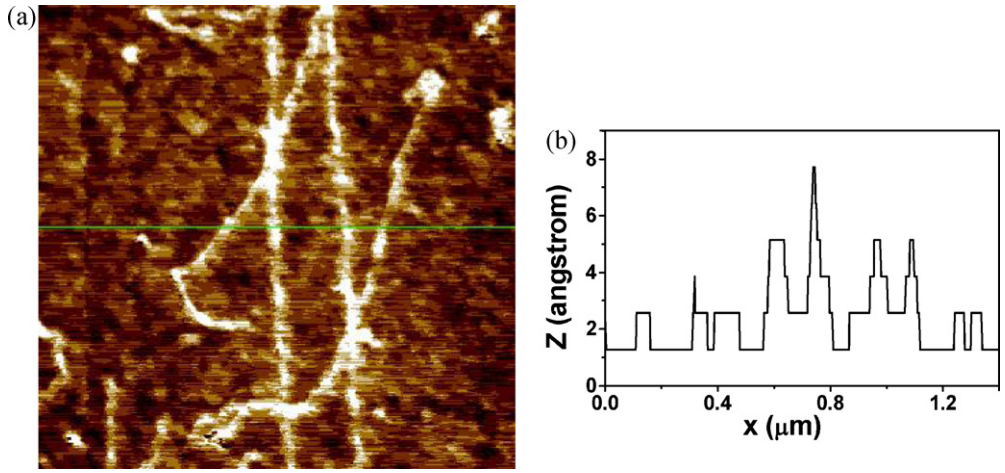

Fig. 4. (a) Topographic image of SSP adsorbed onto Si wafers from dilute solution (0.05 g/L) prepared in pure EmimAc with the corresponding cross-section (b). Scan area 1.5 μm × 1.5 μm, Z = 1.0 nm.

Table 2
Mean thickness values of LYS (d_{LYS}) layers immobilized onto SSP-covered Si wafers (1.0 cm^2).

Solvent for SSP[a]	* γ_S^d (mJ/m^2)	* γ_S^p (mJ/m^2)	* γ_S^{total} (mJ/m^2)	d_{LYS} (nm)	$\Delta\tau$ (%) 1st use	$\Delta\tau$ (%) 2nd use
EmimAc	39 ± 2	29 ± 1	68 ± 2	1.4 ± 0.3	3 ± 1	0
Water	40 ± 2	25 ± 2	65 ± 2	1.6 ± 0.2	54 ± 5	43 ± 5
NaOH 0.01 M	43 ± 3	14 ± 2	57 ± 3	2.0 ± 0.2	45 ± 5	40 ± 4

Dispersive (γ_S^d) and polar (γ_S^p) components of the surface energy were determined for SSP using the geometric mean equation *. γ_S^{total} is the sum of γ_S^d and polar γ_S^p components. $\Delta\tau$ stands for the relative decrease of turbidity due to cell disruption catalyzed by LYS immobilized onto three SSP-covered Si wafers (3.0 cm^2). The same samples were used twice (1st and 2nd use) in order to evaluate re-use possibility and immobilized enzyme stability.

[a] Solvents used for dissolution of SSP and further adsorption onto Si wafers.

2007; Kosaka, Kawano, Salvadori, & Petri, 2005; Maciel, Kosaka, de Paula, Feitosa, & Petri, 2007; Sierakowski, Freitas, Fujimoto, & Petri, 2002; Velzenberger, Kirat, Legeay, Nagel, & Pezron, 2009) or DNA (Sasou, Sugiyama, Ishida, Ohtani, & Miyake, 2009). In this work the effect of surface energy parameters on the immobilization of LYS onto SSP films adsorbed from EmimAc, water and NaH 0.01 mol/L was also investigated. Table 2 shows the mean thickness of LYS (d_{LYS}) layers immobilized onto SSP films adsorbed from each solvent with the corresponding surface energy values. The d_{LYS} values tend to increase with the decrease of γ_S^p and γ_S^{total}. Similar trend was also observed for the adsorption of fibronectin. One possible reason for this effect is the entropic gain due to protein denaturation and hydration water release upon adsorbing onto more hydrophobic surfaces (Haynes & Norde, 1995). If this hypothesis is true, LYS immobilized onto SSP films prepared from NaOH 0.01 mol/L solutions should be less active (more denaturated) than those immobilized onto SSP films prepared from water or EmimAc. Table 2 shows the relative decrease of turbidity due to cell disruption ($\Delta\tau$) catalyzed by LYS immobilized onto SSP films. The largest $\Delta\tau$ value of 54 ± 5% was observed for LYS immobilized onto SSP films adsorbed from water, which have γ_S^p and γ_S^{total} values relatively high. The $\Delta\tau$ values decreased to 45 ± 5% when LYS was immobilized onto SSP films adsorbed from NaOH 0.01 mol/L, which present lower γ_S^p and γ_S^{total} values, keeping the correlation. However, the correlation between $\Delta\tau$ and γ_S^p and γ_S^{total} values was not observed when LYS was immobilized onto SSP films adsorbed from

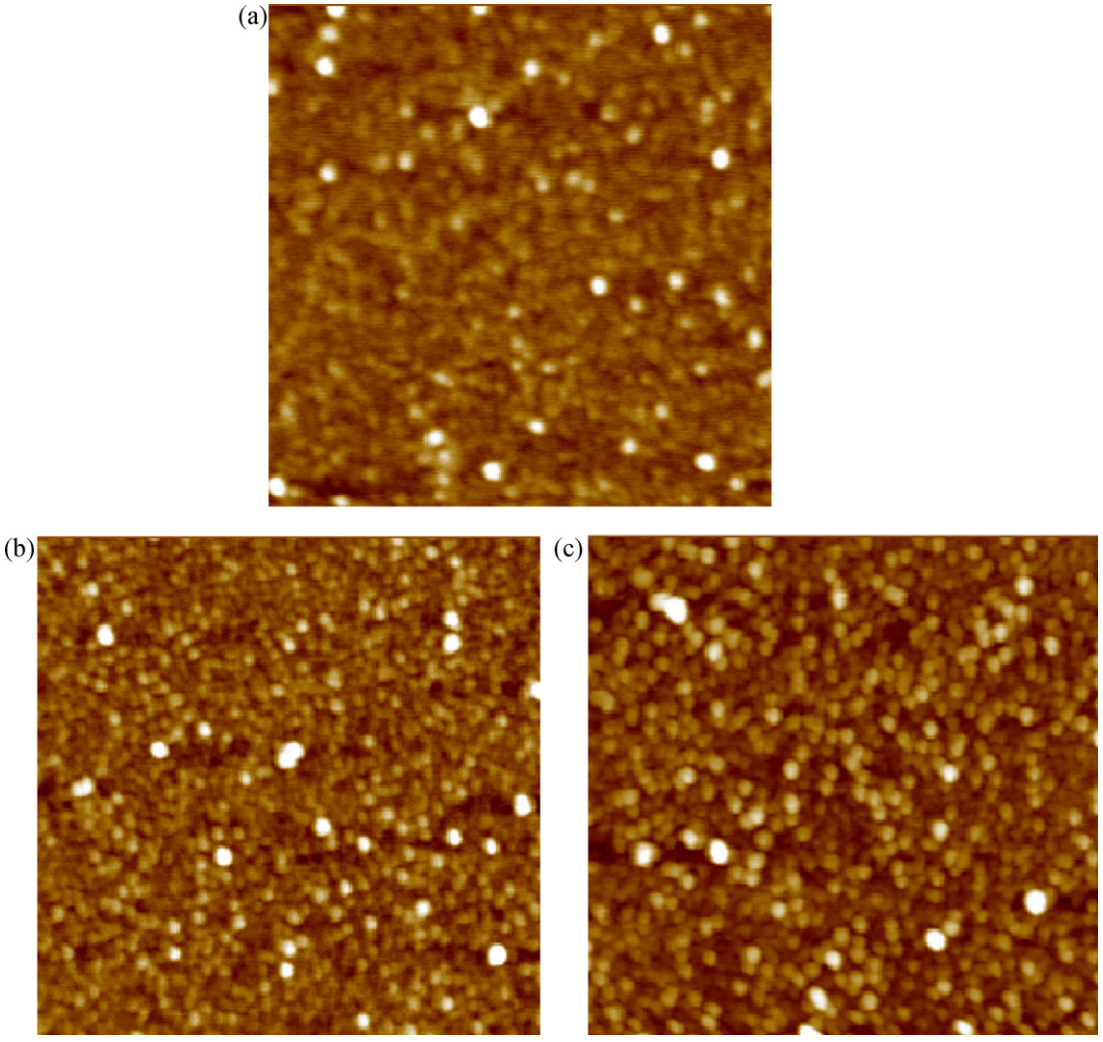

Fig. 5. AFM topographic images (1 μm × 1 μm) obtained for immobilized LYS molecules onto SSP films adsorbed from (a) Emim/Ac, Z = 5.0 nm; (b) water, Z = 5.0 nm or (c) NaOH 0.01 mol/L, Z = 5.0 nm.

EmimAc. In this case, $\Delta\tau$ was almost null (3 ± 1)%. One possible explanation for this result might be LYS denaturation upon contact with EmimAc molecules, which might have not been removed, even after exhaustive rinsing. Ionic liquids are known as denaturing media (Turner, Spear, Huddleston, Holbrey, & Rogers, 2003). AFM image of LYS adsorbed onto SSP films adsorbed from EmimAc (Fig. 5a), water (Fig. 5b) or NaOH (Fig. 5c) revealed LYS molecules as spherical entities distributed similarly on the different support layers. After the first use of LYS-covered SSP films adsorbed from water or NaOH were rinsed with distilled water, dried with N_2 and then the antimicrobial effect was again evaluated. Table 2 shows that the enzymatic activity level decreased only 5–10%, indicating that consecutive re-use of LYS-covered SSP films was successful.

The preservation of LYS native structure is expected when the disulfide bonds are kept intact (Danial, Klok, Norde, & Stuart, 2007), so one can conclude that upon adsorbing LYS onto SSP films adsorbed from water or NaOH disulfide bonds remained partially unchanged. LYS catalytic mechanism involves residues Glu35 and Asp52, which bind to saccharide ring that carry the glycosidic oxygen, so that Glu35 is responsible for acid catalysis and Asp52 for the stabilization of carbonium ion. Hydrophobic residues Trp62 and Trp63 stabilize the flapping (Blake et al., 1965; Danial et al., 2007). Considering LYS catalytic site described above, one can conclude that upon adsorbing LYS onto SSP films, Glu35, Asp52, Trp62 and Trp63 residues are partially preserved. This finding opens the possibility of applying LYS coated SSP films as antimicrobial material for biomedical purposes.

4. Conclusions

In this study the effect of solvent on the morphology and surface properties of adsorbed SSP films was investigated. The use of EmimAc, an ionic liquid, led to smooth SSP surfaces and allowed the visualization of isolated SSP chains. In fact, ionic liquids have proven to be excellent media for polysaccharides dissolution and modification (El Seoud et al., 2007; Swatloski et al., 2002). Nevertheless, EmimAc molecules are not easily removed from SSP films, as evidenced by the high surface energy value $(68 \pm 2\ \mathrm{mJ/m^2})$ and lysozyme denaturation. Surface energy values found for SSP adsorbed from water and NaOH were $65 \pm 2\ \mathrm{mJ/m^2}$ and $57 \pm 3\ \mathrm{mJ/m^2}$, respectively. This small difference was brought about by a reduction of the polar component of surface energy of the latter.

The idea of immobilizing of lysozyme (LYS) onto SSP films was catalyzed by the desire of combining two natural macromolecules to obtain antimicrobial surfaces, which can be applied as packing or coating materials. The results presented here indicated that the activity of immobilized LYS was favored when SSP films presented higher γ_S^p and γ_S^{total} values. Maybe high γ_S^p values help keeping water of hydration on the surface, avoiding enzyme denaturation. Similar studies with other enzymes are under progress in our group. They should provide more data to set a correlation between surface properties and enzymatic activity of immobilized enzymes.

Acknowledgments

The authors thank Rede Nanoglicobiotecnologia CNPq/MCT (Proc # 55.5169/2005-7), FAPESP and CNPq for the financial support.

Appendix A. Supplementary data

Supplementary data associated with this article can be found, in the online version, at doi:10.1016/j.carbpol.2010.02.015.

References

Adamson, W. A. (1990). *Physical chemistry of surfaces*. Toronto: John Wiley & Sons.
Amim Júnior, J., Kosaka, P. M., Petri, D. F. S., Maia, F. C. B., & Miranda, P. B. (2009). Stability and interface properties of thin cellulose ester films adsorbed from acetone and ethyl acetate solutions. *Journal of Colloid and Interface Science*, *332*, 477–483.
Amim Júnior, J., Petri, D. F. S., Maia, F. C. B., & Miranda, P. B. (2009). Solution behavior and surface properties of carboxymethylcellulose acetate butyrate. *Cellulose*, *16*, 773–782.
Azzam, R. M. A., & Bashara, N. M. (1987). *Ellipsometry and polarized light*. Amsterdam: North-Holland.
Bergmeyer, H. U. (1984). H. U. Bergmeyer, J. Bergmeyer, & M. Grals (Eds.), *Methods of enzymatic analysis* (pp. 190–195). Weinheim: Verlag Chemie.
Blake, C. C. F., Koenig, D. F., Mair, G. A., North, A. C. T., Phillips, D. C., & Sarma, V. R. (1965). Structure of hen egg-white lysozyme—A 3-dimensional Fourier synthesis at 2A resolution. *Nature*, *206*, 757–761.
Brito, A. C. F., Sierakowski, M. R., Reicher, F., Paula, R. C. M., & Feitosa, J. P. A. (2005). Dynamic rheological study of *Sterculia striata* and Karaya polysaccharides in aqueous solution. *Food Hydrocolloids*, *19*, 861–867.
Brito, A. C. F., Silva, D. A., Paula, R. C. M., & Feitosa, J. P. A. (2004). *Sterculia striata* exudate polysaccharide: Characterization, rheological properties and comparison with *Sterculia urens* (karaya) polysaccharide. *Polymer International*, *53*, 1025–1032.
Chaudhury, M. K. (1996). Interfacial interaction between low-energy surfaces. *Materials Science Engineering*, *16*, 97–159.
Danial, M., Klok, H. A., Norde, W., & Stuart, M. A. C. (2007). Complex coacervate core micelles with a lysozyme-modified corona. *Langmuir*, *23*, 8003–8009.
Dumitriu, S. (2005). *Polysaccharides: Structural diversity and functional versatility*. New York: Marcel Dekker.
El Seoud, O. A., Koschella, A., Fidale, L. C., Dorn, S., & Heinze, T. (2007). Applications of ionic liquids in carbohydrate chemistry: A window of opportunities. *Biomacromolecules*, *8*, 2629–2647.
Harnett, E. M., Alderman, J., & Wood, T. (2007). The surface energy of various biomaterials coated with adhesion molecules used in cell culture. *Colloids and Surfaces B: Biointerfaces*, *55*, 90–97.
Haynes, C. A., & Norde, W. (1995). Structures and stabilities of adsorbed proteins. *Journal of Colloid and Interface Science*, *169*, 313–328.
Gomes, G. S., Almeida, A. T., Kosaka, P. M., Rogero, S. O., Cruz, A. S., Ikeda, T. I., et al. (2007). Cellulose acetate propionate coated titanium: Characterization and biotechnological application. *Materials Research*, *10*, 469–474.
Kontturi, E., Johansson, L.-S., Kontturi, K. S., Ahonen, P., Thüne, P. C., & Laine, J. (2007). Cellulose nanocrystal submonolayers by spin coating. *Langmuir*, *23*, 9674–9680.
Kosaka, P. M., Kawano, Y., El Seoud, O. A., & Petri, D. F. S. (2007). Catalytic activity of lipase immobilized onto ultrathin films of cellulose esters. *Langmuir*, *23*, 12167–12173.
Kosaka, P. M., Kawano, Y., Salvadori, M. C., & Petri, D. F. S. (2005). Characterization of ultrathin films of cellulose esters. *Cellulose*, *12*, 351–359.
Maciel, J. S., Kosaka, P. M., de Paula, R. C. M., Feitosa, J. P. A., & Petri, D. F. S. (2007). Formation of cashew gum thin films onto silicon wafers or amino-terminated surfaces and the immobilizations of concanavalin A on them. *Carbohydrate Polymers*, *69*, 522–529.
Marmur, A. (2006). Soft contact: Measurement and interpretation of contact angles. *Soft Matter*, *2*, 12–17.
McKenzie, H. A., & White, H. A. (1991). Lysozyme and alpha-lactalbumin—structure, function, and interrelationships. *Advances in Protein Chemistry*, *41*, 173–315.
Ortega-Vinuesa, J. L., Tengvall, P., & Lundstrom, I. (1998). Molecular packing of HSA, IgG, and fibrinogen adsorbed on silicon by AFM imaging. *Thin Solid Films*, *324*, 257–273.
Owens, D. K., & Wendt, R. C. (1969). Estimation of the surface free energy of polymers. *Journal of Applied Polymer Science*, *13*, 1741–1747.
Palik, E. D. (1985). *Handbook of optical constants of solids*. London: Academic Press.
Petri, D. F. S., Wenz, G., Schunk, P., & Schimmel, T. (1999). An improved method for the assembly of amino-terminated monolayers on SiO2 and the vapor deposition of gold layers. *Langmuir*, *15*, 4520–4523.
Sasou, M., Sugiyama, S., Ishida, T., Ohtani, T., & Miyake, K. (2009). Influence of the surface free energy of silane-coupled mica substrate on the fixing and straightening of DNA. *Thin Solid Films*, *517*, 4425–4431.
Shimizu, R. N., & Demarquette, N. R. (2000). Evaluation of surface energy of solid polymers using different models. *Journal of Applied Polymer Science*, *76*, 1831–1845.
Sierakowski, M. R., Freitas, R. A., Fujimoto, J., & Petri, D. F. S. (2002). Adsorption behavior of oxidized galactomannans onto amino-terminated surfaces and their interaction with bovine serum albumin. *Carbohydrate Polymers*, *49*, 167–175.
Silva, D. A., Brito, A. C. F., Paula, R. C. M., Feitosa, J. P. A., & Paula, H. C. B. (2003). Effect of mono and divalent salts on gelation of native, Na and deacetylated *Sterculia striata* and *Sterculia urens* polysaccharide gels. *Carbohydrate Polymers*, *54*, 229–236.
Swatloski, R. P., Spear, S. K., Holbrey, J. D., & Rogers, R. D. (2002). Dissolution of cellose with ionic liquids. *Journal of the American Chemical Society*, *124*, 4974–4975.
Turner, M. B., Spear, S. K., Huddleston, J. G., Holbrey, J. D., & Rogers, R. D. (2003). Ionic liquid salt-induced inactivation and unfolding of cellulase from *Trichoderma reesei*. *Green Chemistry*, *5*, 443–447.
Velzenberger, E., Kirat, K. E., Legeay, G., Nagel, M. D., & Pezron, I. (2009). Characterization of biomaterials polar interactions in physiological conditions using

liquid–liquid contact angle measurements. Relation to fibronectin adsorption. *Colloids and Surfaces B-Biointerfaces*, *68*, 238–244.

Wiegand, G., Jaworek, T., Wegner, G., & Sackmann, E. (1997). Heterogeneous surfaces of structured hairy-rod polymer films: Preparation and methods of functionalization. *Langmuir*, *13*, 3563–3569.

Zampa, M. F., Brito, A. C. F., Kitagawa, I. L., Constantino, C. J. L., Oliveira Júnior, O. N., Cunha, H. N., et al. (2007). Natural gum-assisted phthalocyanine immobilization in electroactive nanocomposites: Physicochemical characterization and sensing applications. *Biomacromolecules*, *8*, 3408–3413.